Supplemental Data

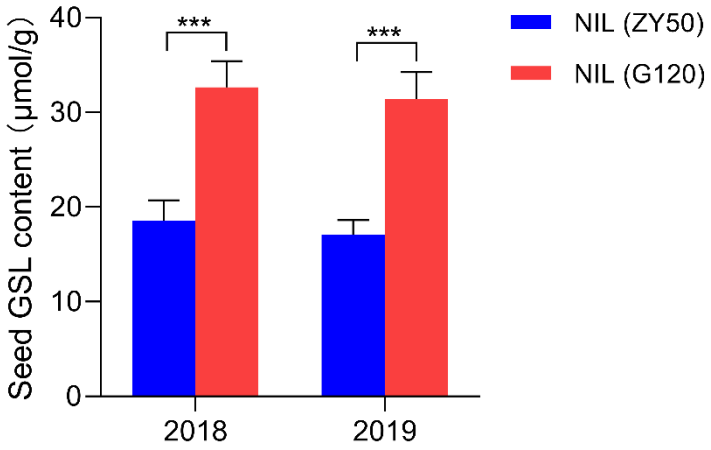

Supplementary Figure S1. Comparison of seed GSL content between NIL(ZY50) and NIL(G120). A two-tailed Student's *t*-test between NIL(ZY50) and NIL(G120) was used to calculate the *P* value. The data represent the mean ± SD ($n \geq 10$), ***$P < 0.001$. 2018 and 2019 represents plants in 2017-2018 and 2018-2019 growing season, respectively. GSL, glucosinolate; NIL, near-isogenic lines.

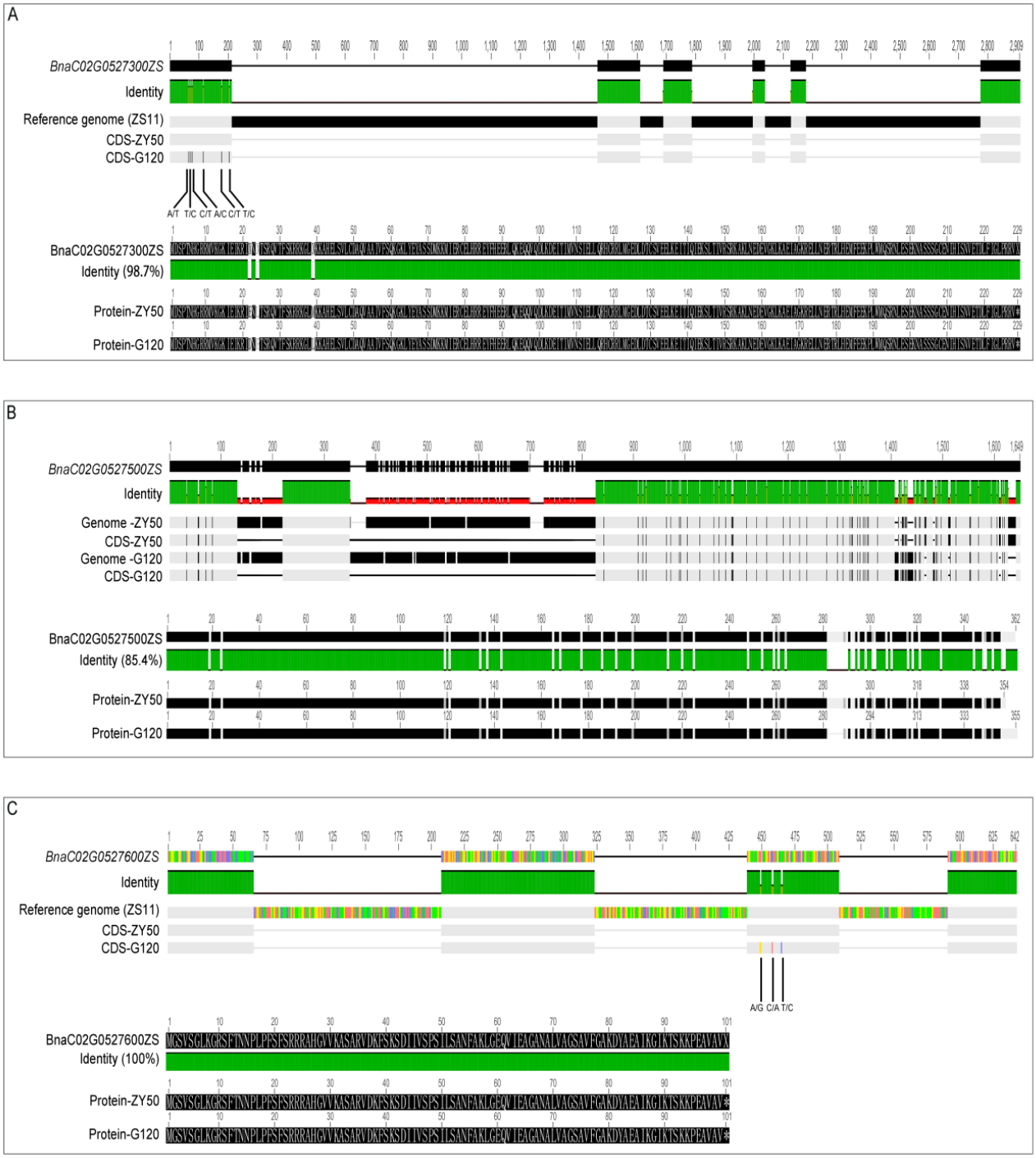

Supplementary Figure S2. Comparison of coding sequences and amino acid sequences of candidate genes between parental lines. (A — C) Comparison of coding sequences and amino acid sequences of *BnaC02G0527300ZS*, *BnaC02G0527500ZS* and *BnaC02G0527600ZS*, respectively, between parental lines.

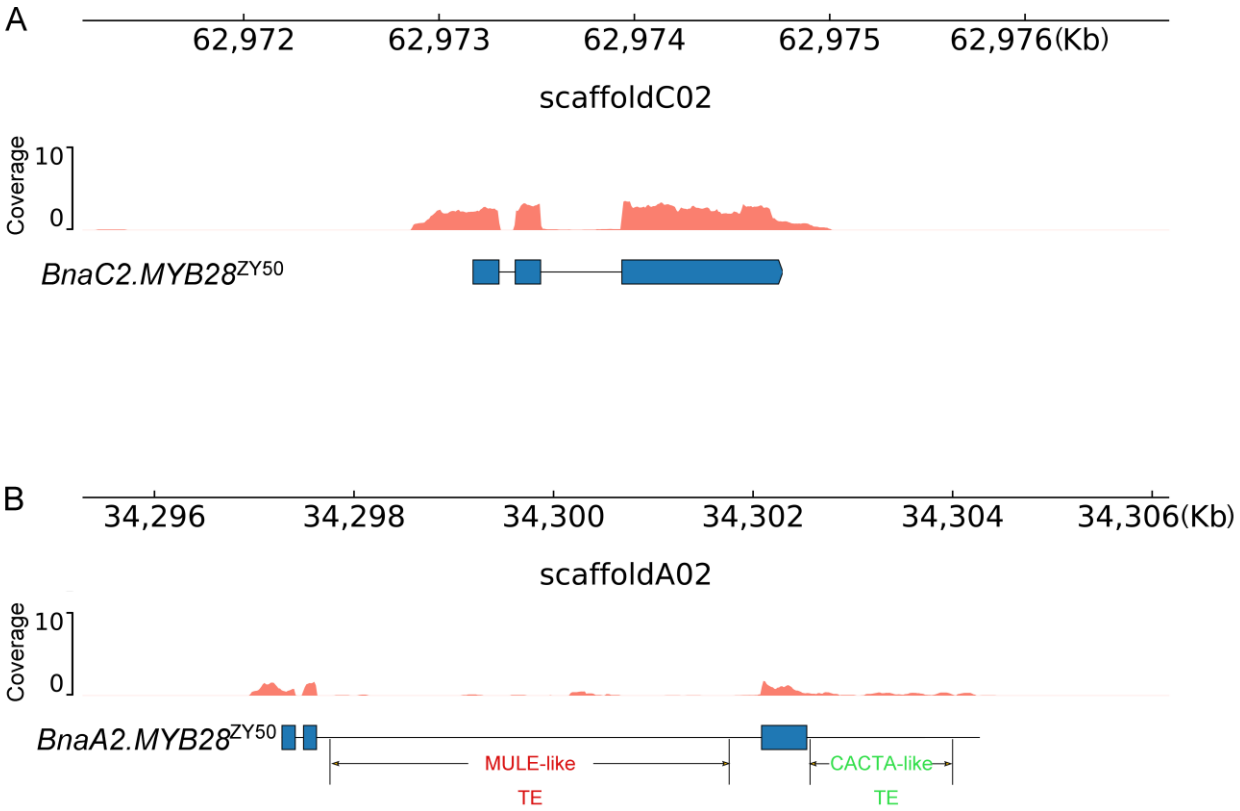

Supplementary Figure S3. Integrative genomics viewer (IGV) displays the transcripts of *BnaC2.MYB28*^{ZY50} and *BnaA2.MYB28*^{ZY50}. (A) Part of the alignment tracks of RNA-seq reads in the region of *BnaC2.MYB28*. (B) Part of the alignment tracks of RNA-seq reads in the region of *BnaA2.MYB28*. Kb, kilobase.

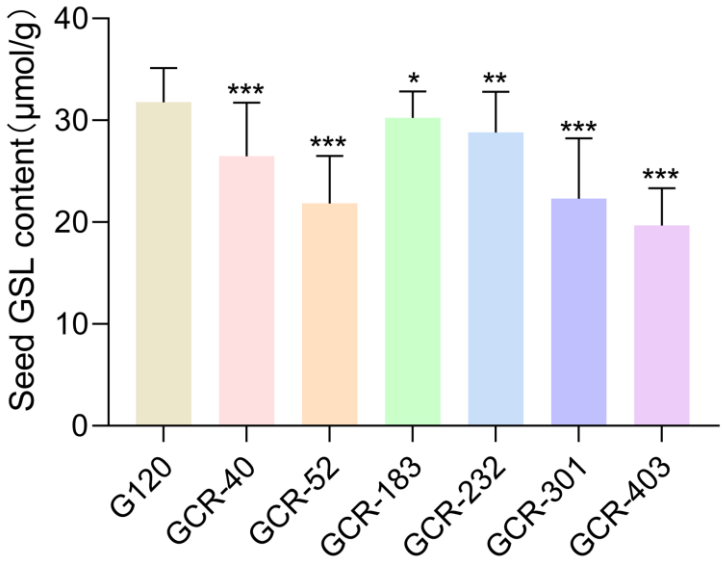

Supplementary Figure S4. SGC of *BnaC2.MYB28*^{G120}-sgRNA plants in the T_1 generation. A two-tailed Student's *t* test between G120 and *BnaC2.MYB28*^{G120}-sgRNA plants was used to calculate the *P* value. The data represent the means ± SD ($n \geq 8$); asterisks indicate significant differences (*t*-test; **P* < 0.05, ***P* < 0.01, ****P* < 0.001). GSL, glucosinolate.

Supplementary Figure S5. Comparison of the promoter sequences of *BnaC2.MYB28* between the parental lines.

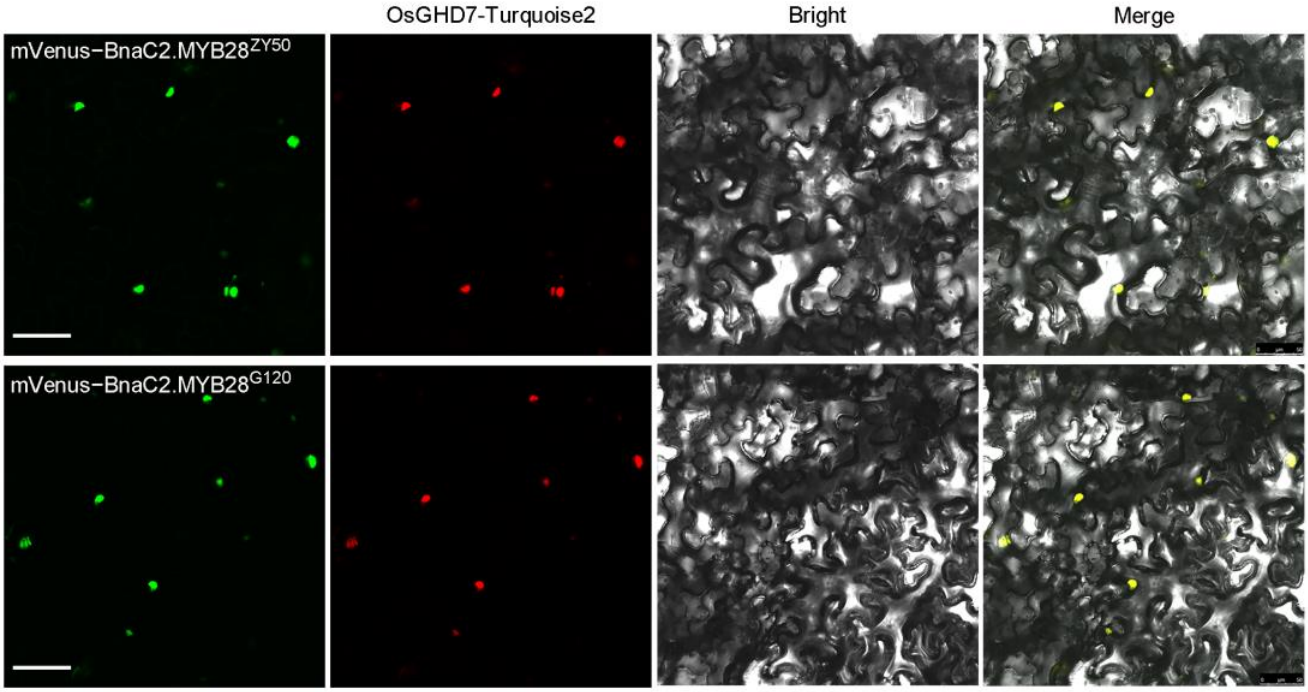

Supplementary Figure S6. Subcellular localization of BnaC2.MYB28 in *Nicotiana benthamiana* leaves. The nuclear protein OsGHD7 fused with Turquoise2 was used as a nuclear marker. Bars = 50 μm.

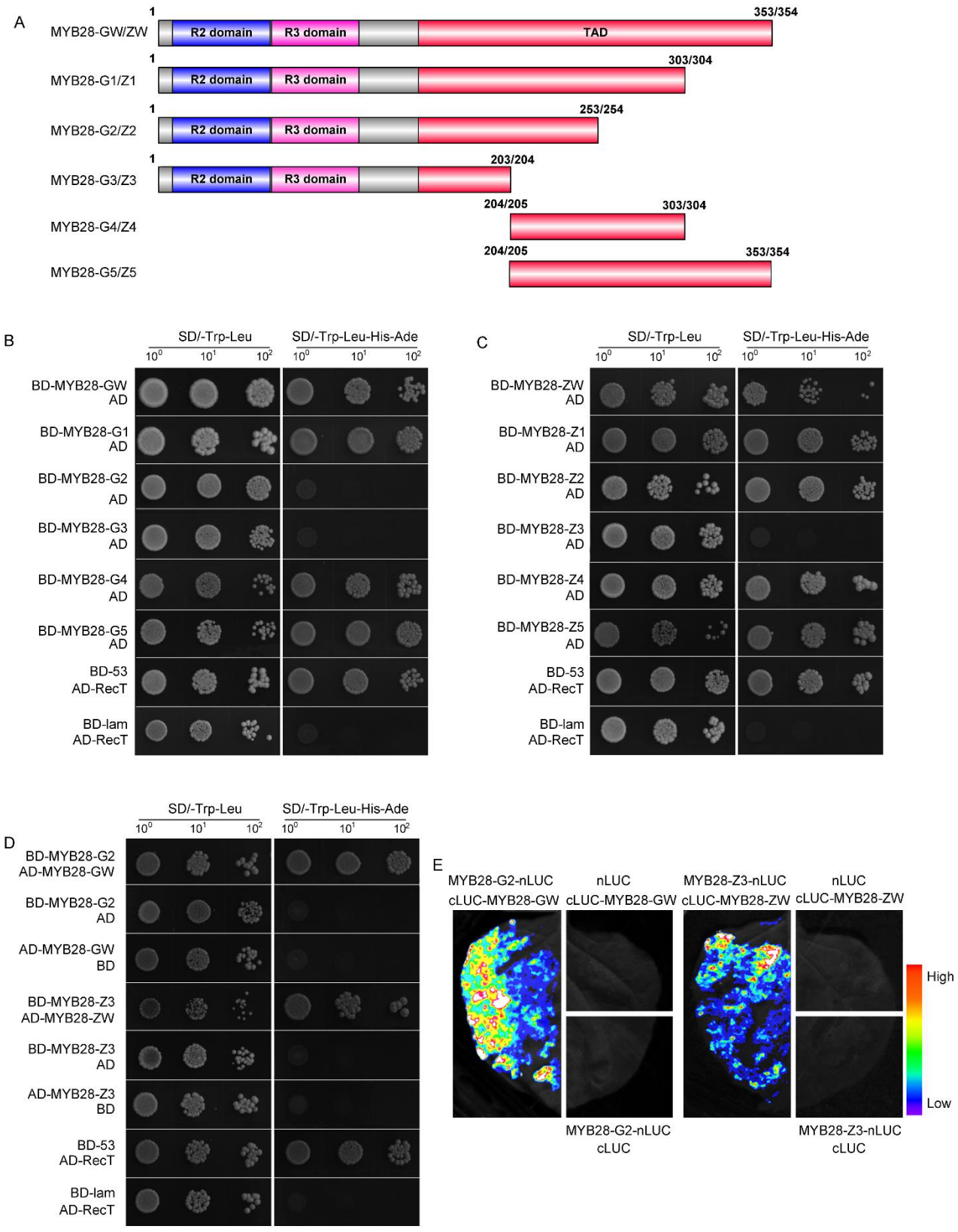

Supplementary Figure S7. Functional regions of BnaC2.MYB28. (A) Schematic diagram showing the various fragments of BnaC2.MYB28. MYB28-GW and MYB28-ZW indicate the whole length of BnaC2.MYB28^{G120} and BnaC2.MYB28^{ZY50} protein, respectively. Transcriptional self-activation test of BnaC2.MYB28^{G120} (B) and BnaC2.MYB28^{ZY50} (C) in yeast-two-hybrid assays. BnaC2.MYB28 forms

homodimers in yeast-two-hybrid (D) and SLC analysis (E). BD-53/AD-RecT was the positive control, and BD-Lam/AD-RecT was the negative control. AD, pGADT7/activation domain; BD, pGBKT7/binding domain; Ade, adenine; His, histidine; Lam, human lamin C; Leu, leucine; RecT, recombination of the SV40 large T antigen; SD, synthetic defined medium; Trp, tryptophan.

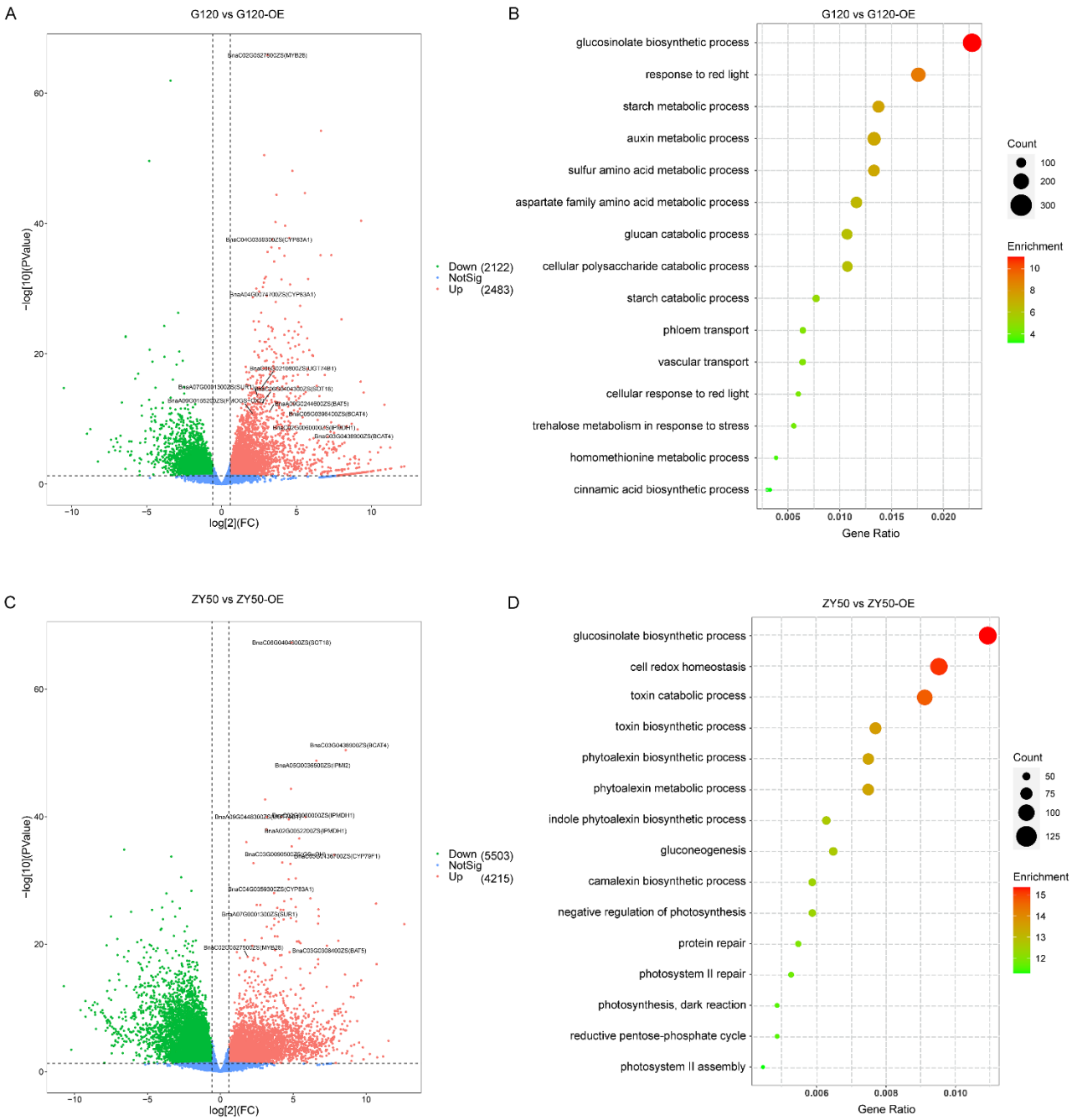

Supplementary Figure S8. RNA-seq analysis between parental lines and *BnaC2.MYB28* overexpressing lines. (A) Volcano plot of gene expression between G120 and its *BnaC2.MYB28* overexpressing line G120-OE (fold change (FC) ≥ 2; *P* value < 0.05). (B) GO analysis of differentially expressed genes between G120 and G120-OE. (C) Volcano plot of gene expression between ZY50 and its *BnaC2.MYB28* overexpressing line ZY50-OE (fold change (FC) ≥ 2; *P* value < 0.05). (D) GO analysis of differentially expressed genes between ZY50 and ZY50-OE.

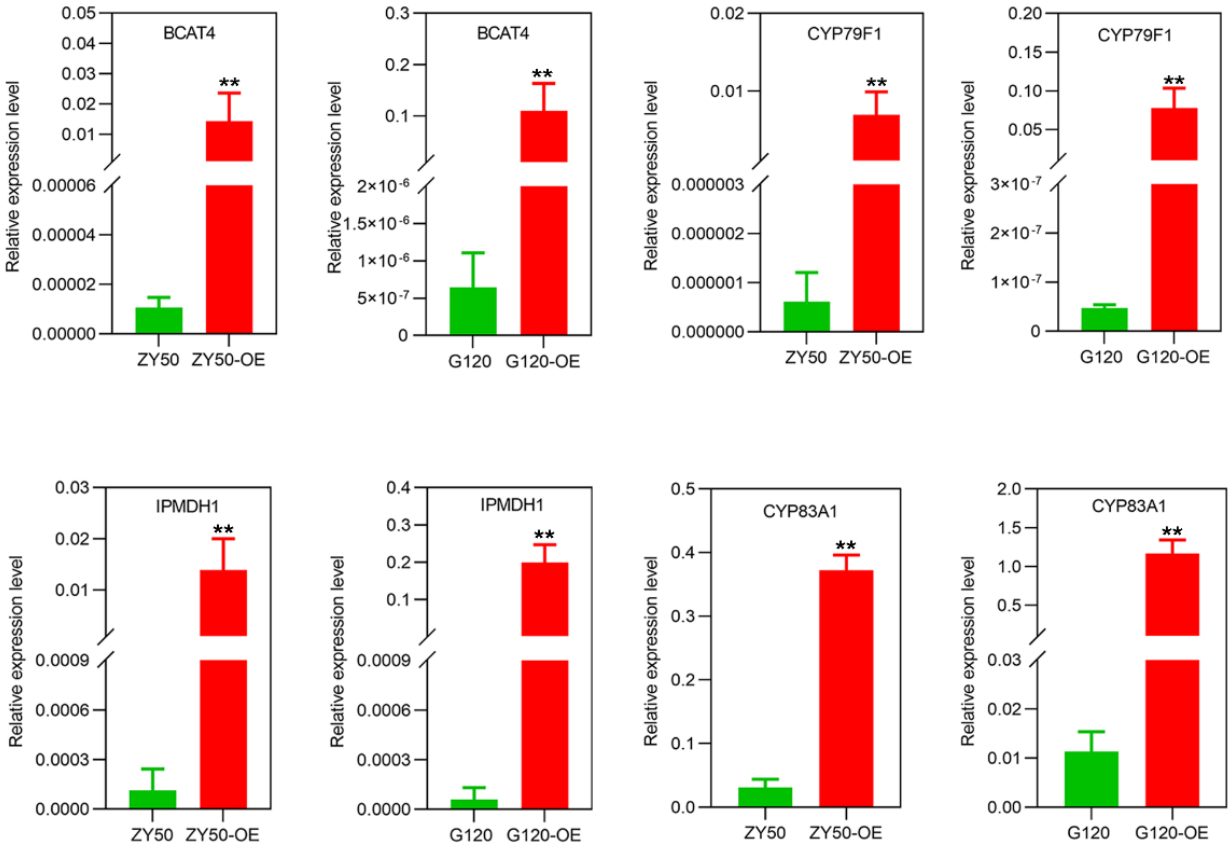

Supplementary Figure S9. RT-qPCR confirmation of the differentially expressed genes involved in GSL biosynthesis obtained by RNA-seq. Error bars represent standard errors from three independent RNA samples. A two-tailed Student's *t*-test was used to generate the *P* values. $^{**}P < 0.01$.

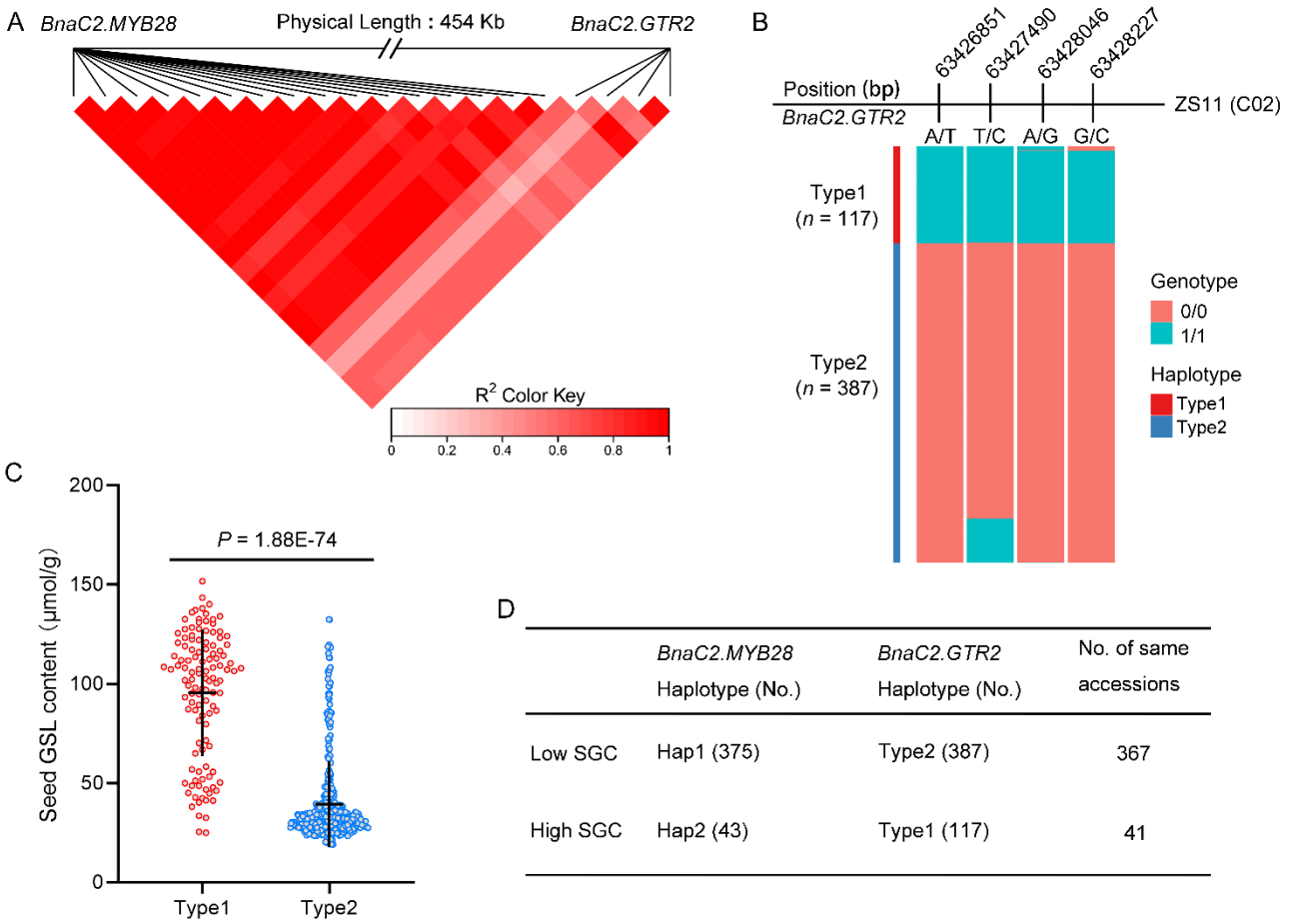

	BnaC2.MYB28 Haplotype (No.)	*BnaC2.GTR2* Haplotype (No.)	No. of same accessions
Low SGC	Hap1 (375)	Type2 (387)	367
High SGC	Hap2 (43)	Type1 (117)	41

Supplementary Figure S10. Co-selection analysis of *BnaC2.MYB28* and *BnaC2.GTR2* in natural population. (A) LD analysis between *BnaC2.MYB28* and *BnaC2.GTR2*. Kb, kilobase. (B) Two major haplotypes were identified in the *BnaC2.GTR2* gene regions. bp, base pair. (C) SGC of the two haplotypes. The horizontal and vertical lines represent the mean value and standard deviation, respectively. Each colored dot represents an individual plant. Data are shown as mean ± SD ($n \geq 117$). A two-tailed Student's *t*-test was used to generate the *P* values. (D) Accession statistics of *BnaC2.MYB28* and *BnaC2.GTR2* haplotypes.

Table S1. SGC in *BnaC2.MYB28*^{G120}-transgenic T_1 lines.

Transgenic line	Mean ± SD		No. of plants		*P*-Value[a]
	Negative	Positive	Negative	Positive	
ZG−4	17.5 ± 1.8	24.6 ± 2.1	14	28	9.07E-14
ZG−8	18.3 ± 2.1	23.2 ± 1.7	11	35	9.35E-10
ZG−13	18.9 ± 2.5	25.3 ± 2.7	10	29	1.01E-07

Data are shown as mean ± SD ($n \geq 10$). *P* values were generated by a two-tailed Student's *t*-test. SD, standard deviation.

[a] indicates the *P* value calculated between negative and positive plants.

Table S2. SGC in *BnaC2.MYB28*-CRISPR T_2 lines.

Transgenic line	Mean ± SD	No. of plants	*P*-Value[a]
G120	32.5 ± 2.7	28	
GCR-52-2	23.9 ± 3.2	26	8.51E-15
GCR-52-3	21.7 ± 2.5	39	1.70E-25
GCR-52-6	24.1 ± 3.3	43	3.51E-17
GCR-403-16	14.1 ± 2.4	32	1.84E-35
GCR-403-17	16.5 ± 2.0	40	1.08E-38
GCR-403-35	15.6 ± 2.4	43	2.94E-39

Data are shown as mean ± SD ($n \geq 26$). *P* values were generated by a two-tailed Student's *t*-test. SD, standard deviation

[a] indicates the *P* value calculated between transgenic lines and G120 plants.

Table S3. SGC in *BnaC2.MYB28*^{ZY50}-transgenic T_1 lines.

Transgenic line	Mean ± SD		No. of plants		*P*-Value[a]
	Negative	Positive	Negative	Positive	
GZ−2	32.6 ± 1.4	40.6 ± 2.3	11	36	6.11E-14
GZ−5	30.7 ± 2.1	37.2 ± 2.1	13	27	2.38E-11
GZ−6	32.2 ± 2.3	44.3 ± 3.2	10	23	5.61E-12

Data are shown as mean ± SD ($n \geq 10$). *P* values were generated by a two-tailed Student's *t*-test. SD, standard deviation.

[a] indicates the *P* value calculated between negative and positive plants.

Table S4. SGC in two p35S::*BnaC2.MYB28*^{ZY50}-transgenic T_1 lines.

Transgenic line	Mean ± SD		No. of plants		*P*-Value[a]
	Negative	Positive	Negative	Positive	
ZOE−22	22.3 ± 3.6	47.9 ± 20.0	9	6	0.002
ZOE−25	19.8 ± 1.1	161.3 ± 15.8	14	46	2.04E-39

Data are shown as mean ± SD ($n \geq 6$). *P* values were generated by a two-tailed Student's *t*-test. SD, standard deviation.

[a] indicates the *P* value calculated between negative and positive plants.

Table S5. SGC in RNAi and overexpressing of *BnaC2.MYB28*^{G120}-transgenic T_0 lines.

Transgenic line	Mean ± SD		No. of plants		*P*-Value[a]
	Negative	Positive	Negative	Positive	
G120−RNAi	33.4 ± 3.1	23.7 ± 2.0	17	6	4.22E-07
G120−OE	32.3± 5.0	128.7 ± 35.9	40	16	4.09E-23

Data are shown as mean ± SD ($n \geq 6$). *P* values were generated by a two-tailed Student's *t*-test. SD, standard deviation.

[a] indicates the *P* value calculated between negative and positive plants.

Table S6. Overlapping genes involved in GSL biosynthesis of ChIP-seq and RNA-seq.

Gene ID (ZS11)	Gene name	*Arabidopsis* locus ID	Description
BnaC03G0321400ZS	*AOP1*	*AT4G03070*	Encodes a possible 2-oxoglutarate-dependent dioxygenase that is involved in glucosinolate biosynthesis.
BnaA02G0257300ZS	*AOP3*	*AT4G03050*	Encodes a 2-oxoglutarate-dependent dioxygenase which is involved in glucosinolate biosynthesis.
BnaA03G0259200ZS *BnaA09G0244600ZS* *BnaC03G0308400ZS* *BnaC03G0308500ZS* *BnaC09G0288000ZS*	*BAT5*	*AT4G12030*	Involved in the transport of 2-keto acids between chloroplasts and the cytosol.
BnaA03G0359600ZS *BnaA05G0362200ZS* *BnaC03G0438900ZS* *BnaC05G0396400ZS*	*BCAT4*	*AT3G19710*	Involved in the methionine chain elongation pathway that leads to the ultimate biosynthesis of methionine-derived glucosinolates.
BnaA08G0192100ZS	*CYP79B1*	*AT4G39950*	Belongs to cytochrome P450 and is involved in tryptophan metabolism.
BnaA04G0074700ZS *BnaC04G0359300ZS*	*CYP83A1*	*AT4G13770*	Encodes a cytochrome p450 enzyme that catalyzes the initial conversion of aldoximes to thiohydroximates in the synthesis of glucosinolates not derived from tryptophan.
BnaA09G0155300ZS *BnaC09G0170500ZS*	*FMO$_{GS-OX1}$*	*AT1G65860*	Belongs to the flavin-monooxygenase (FMO) family.
BnaA09G0155200ZS	*FMO$_{GS-OX2}$*	*AT1G62540*	Belongs to the flavin-monooxygenase (FMO) family.
BnaC03G0090500ZS	*GS-OH*	*AT2G25450*	Encodes a 2-oxoacid-dependent dioxygenase involved in the production of 2-hydroxybut-3-enyl glucosinolate.
BnaA02G0052200ZS *BnaC02G0060000ZS*	*IPMDH1*	*AT5G14200*	Involved in glucosinolate biosynthesis, in methionine chain elongation.
BnaA05G0036500ZS	*IPMI2*	*AT2G43100*	Together with IPMI SSU3 participates in the Met chain elongation pathway.
BnaA06G0128100ZS *BnaC05G0156200ZS*	*SOT17*	*AT1G18590*	Encodes a desulfoglucosinolate sulfotransferase, involved in the final step of glucosinolate core structure biosynthesis.
BnaC06G0404300ZS	*SOT18*	*AT1G74090*	Encodes a desulfoglucosinolate sulfotransferase, involved in the final step of glucosinolate core structure biosynthesis.
BnaA07G0001300ZS *BnaC07G0005900ZS*	*SUR1*	*AT2G20610*	Encodes a C-S lyase involved in converting S-alkylthiohydroximate to thiohydroximate in glucosinolate biosynthesis.
BnaA09G0448300ZS *BnaC05G0210800ZS*	*UTG74B1*	*AT1G24100*	Encodes a UDP-glucose: thiohydroximate S-glucosyltransferase, involved in glucosinolate biosynthesis.

Table S7. Summary of primers used in this study.

Primer name	Sequence 5′-3′	Purpose
SSA2-102F	AGCAAAAGCACCTCATTAGC	Fine mapping (co-segregation marker of *qGSL-C2*)
SSA2-102R	TCCCAGCGTGAATTGAACCTA	
SSA2-146F	GGTTAATCCACCATGATGTC	Fine mapping (flanking marker of *qGSL-C2*)
SSA2-146R	GCTAAGATTGTTAGAGCGTTCC	
SSA2-157F	ACTCTCTAGCCACCAAGTCCA	Fine mapping (flanking marker of *qGSL-C2*)
SSA2-157R	ACACCGAAAAACTTGCGACTGCT	
G120-pM999F	GGAGAGGACAGGGTACCCGGGATGTCAAGAAAGCCATGTTGT	*BnaC2.MYB28*^{G120}-GFP construction
G120-pM999R	GGCAGCGGCAGCAGCCGGATCCTATGAAATCATAGTCCGTGTCA	
ZY50-pM999F	GGAGAGGACAGGGTACCCGGGATGTCAAGAAAGCCATGTTGT	*BnaC2.MYB28*^{ZY50}-GFP construction
ZY50-pM999R	GGCAGCGGCAGCAGCCGGATCCTATGATTTGCTTATCGAAGAAATC	
qBCAT4-F	GGATAACATTAGCAGAGGCGA	RT-qPCR analysis of *BnaBCAT4* expression
qBCAT4-R	TTCCTCAACCTTGTAGCCGA	
qIPMDH1-F	TTCCATCTGCTAGTCTCGGT	RT-qPCR analysis of *BnaIPMDH1* expression
qIPMDH1-R	CATCCCACCAGTTTATTTCCAG	
qCYP79F1-F	ATTTCATTCCCAAAGGTAGCCAC	RT-qPCR analysis of *BnaCYP79F1* expression
qCYP79F1-R	AGAAAGCTCCTTCGAGATTCC	
qCYP83A1-F	AGATCAACCTTTCGCCTCCAAG	RT-qPCR analysis of *BnaCYP83A1* expression
qCYP83A1-R	ACTTCATCAAATACGTCATTCCCCA	
qBnACTIN7-L	CCCTGGAATTGCTGACCGTA	RT-qPCR control for *B. napus*
qBnACTIN7-R	TGGAAAGTGCTGAGGGATGC	
qBnaC2.MYB28-F	CATCATGCTCCATGCTGCTC	RT-qPCR analysis of *BnaC2.MYB28* expression
qBnaC2.MYB28-R	AGAAGCTAGTGGCTTGTGAGTCAC	
G120- DT1-BsF	ATATATGGTCTCGATTGGTGTGGTGATCTCGGAAACGTT	CRISPR/Cas9 construction of *BnaC2.MYB28*^{G120}
G120-F0	TGGTGTGGTGATCTCGGAAACGTTTTAGAGCTAGAAATAGC	

G120-DT2-R0	AACGCCCTCGAAGTTTCCTATCCAATCTCTTAGTCGACTCTAC	CRISPR/Cas9 construction of *BnaC2.MYB28*^{G120}
G120-DT2-BsR	ATTATTGGTCTCGAAACGCCCTCGAAGTTTCCTATCCAA	
LUC-ZY50F	CTATAGGGCGAATTGGGTACCATATGTGAGGGGTGGTAAGAGACG	Promoter activity analysis of *BnaC2.MYB28*^{ZY50}
LUC-ZY50R	CGCTCTAGAACTAGTGGATCCTTTCTCCGATATATATATATGAACAC	
LUC-G120F	CTATAGGGCGAATTGGGTACCCCGGATATCCATAAACCTTCG	Promoter activity analysis of *BnaC2.MYB28*^{G120}
LUC-G120R	CGCTCTAGAACTAGTGGATCCTTTCTCCGATATATATAGATGAAC	
35S-G120F	CAGGTCGACTCTAGAGGATCCATGTCAAGAAAGCCATGTTGTGT	35S::*BnaC2.MYB28*^{G120} construction
35S-G120R	CGAGAATTCGAGCTCGGTACCTCATATGAAATCATAGTCCGTGTCA	
35S-ZY50F	CAGGTCGACTCTAGAGGATCCATGTCAAGAAAGCCATGTTGTGT	35S::*BnaC2.MYB28*^{ZY50} construction
35S-ZY50R	CGAGAATTCGAGCTCGGTACCTCATATGATTTGCTTATCGAAGAAATC	
HB-G120F	TATGACCATGATTACGAATTCCCGGATATCCATAAACCTTCGAAG	Functional analysis for *BnaC2.MYB28*^{G120}
HB-G120R	CAGGTCGACTCTAGAGGATCCGACGATAAGAACCTTTGCGAGATC	
HB-ZY50F	TATGACCATGATTACGAATTCATATGTGAGGGGTGGTAAGAGACG	Functional analysis for *BnaC2.MYB28*^{ZY50}
HB-ZY50R	CAGGTCGACTCTAGAGGATCCCGGCTCACACTTCCGATTATCTG	
MR-G120F1	TTACAATTACCATGGGGCGCGCCCCAATGGCTTCCCTGAG	RNAi construction of *BnaC2.MYB28*^{G120}
MR-G120R1	AAGAAATTCTTACACATTTAAATTACTCGACATTCGTATTGTGC	
MR-G120F2	AATTTGCAGGTATTTGGATCCTACTCGACATTCGTATTGTGC	RNAi construction of *BnaC2.MYB28*^{G120}
MR-G120R2	ACTCTAGGGACTAGTCCCGGGCCAATGGCTTCCCTGAG	
CR-gF1	CATGTCTCTTCCTCTTTCCT	Detection primer of target 1 for CRISPR construction
CR-gR1	AGCCTTGATGTAGAGCTCGA	
CR-gF2	CTAGATGCATCTAGTTCCGA	Detection primer of target 2 for CRISPR construction
CR-gR2	AACCTCTCTGAACTGGTGTG	